Low-energy photodisintegration of ⁹Be with the molecular orbit model

N. Itagaki 1* and K. Hagino 2†

¹Department of physics, University of Tokyo, Hongo, Tokyo 113-0033, Japan

² Yukawa Institute for Theoretical Physics,

Kyoto University, Kyoto 606-8502, Japan

(Dated: November 5, 2018)

Abstract

We use a microscopic three-cluster model with the $\alpha + \alpha + n$ configuration to analyze with astrophysical interests the photodisintegration cross section of ${}^{9}\text{Be}$. The valence neutron in ${}^{9}\text{Be}$ is treated in the molecular orbit model (MO), including continuum states by the box discretization method. It is shown that good agreement is achieved with the recently measured B(E1) transition probability from the ground state to the first $1/2^{+}$ state when the box size is enlarged, resulting in reasonable reproduction of the experimental data for the photodisintegration cross section. The Coulomb dissociation of ${}^{9}\text{Be}$ is also discussed.

PACS numbers: 21.60.Gx,25.20.-x,27.20.+n,26.30.+k

 $^{{\}rm *Electronic~address:~itagaki@phys.s.u-tokyo.ac.jp}$

[†]Electronic address: hagino@yukawa.kyoto-u.ac.jp

The ⁹Be nucleus has been popular especially for the past few years. Firstly, it has been often used as a target for projectile fragmentation reactions which involve the radioactive beams [1]. In order to analyze the experimental data, a new neutron-⁹Be optical potential was also constructed [2]. Secondly, the nucleus has been utilized to investigate the role of break-up process in heavy-ion subbarrier fusion reactions [3, 4]. It was reported in Ref. [3] that the complete fusion cross sections for the ⁹Be + ²⁰⁸Pb reaction were hindered by 68% at energies above the Coulomb barrier compared with those expected from a simple one dimensional potential model. This large suppression of complete fusion cross sections was attributed to the low energy thresholds for breakup of ⁹Be into charged fragments, i.e., Q = -1.57 MeV for ⁹Be $\rightarrow \alpha + \alpha + n$ and Q = -2.47 MeV for ⁹Be $\rightarrow \alpha + ^5$ He. The subbarrier breakup reaction of ⁹Be was also measured subsequently, observing large α particle cross sections even at energies well below the Coulomb barrier [4].

⁹Be is interesting also from the nuclear structure point of view [5, 6, 7, 8, 9]. The prominent α cluster structure is well established for this nucleus, and furthermore, it is a loosely bound nucleus in a sense that none of the two-body subsystems (α - α or α -n) is particle stable. These properties make ⁹Be a good testing ground for any nuclear structure model applying to heavier Be isotopes. Based on a similar idea as the linear combination of atomic orbitals (LCAO) for hydrogen molecules in quantum chemistry, the molecular orbit model (MO) was developed for the ⁹Be nucleus[5]. This model has recently been applied with success to other heavier isotopes as well [9, 10, 11, 12]. For instance, it was pointed out that the presence of valence neutrons enhances the α cluster structure of ¹⁰Be by occupying the $1/2^+$ (σ -) orbit in the sd-shell [9].

Another important aspect of the ${}^9\mathrm{Be}$ nucleus is its role in the r-process nucleosynthesis for heavier elements in the neutrino-driven wind formed in core-collapse supernovae. In such an exploding environment with abundant neutrons, the three-body reaction $\alpha(\alpha n, \gamma){}^9\mathrm{Be}$, followed by ${}^9\mathrm{Be}(\alpha, n){}^{12}\mathrm{C}$, plays a key role to bridge the unstable mass gaps at A=5 and 8 compared with the triple- α reaction [13, 14]. The reaction rate for the former process is governed by the low energy resonances of ${}^9\mathrm{Be}$, which can be determined experimentally by measuring the cross section for the inverse reaction, i.e., the photodisintegration process ${}^9\mathrm{Be}(\gamma,\alpha n)\alpha$ [14]. Utsunomiya et~al. recently performed such measurement using laser-induced Compton backscattered γ rays [15]. They obtained the B(E1) transition probability from the ground $3/2^-$ state to the first $1/2^+$ state (the first excited state) almost twice as

large as the previous measurement which used inelastic electron scattering, and the resonance energy of the first $1/2^+$ state which is slightly shifted upperward by 0.064 MeV [15].

From the theoretical point of view, the treatment of the $1/2^+$ state in ${}^9\text{Be}$ has been a challenge, since it is not bound but lies above the ${}^8\text{Be}+n$ threshold only by 19 keV ($E_x=1.68$ MeV). The aim of this paper is to present a detailed analysis of this state based on the molecular orbit method, and apply it to the photodisintegration of ${}^9\text{Be}$ in order to analyze the new experimental data of Utsunomiya et al.. Although Descouvement has done similar studies based on a microscopic three-cluster model and obtained nice agreement with the experimental data for the B(E1) value as well as the photodisintegration cross sections [16], we particularly focus on the dependence of the B(E1) value on the properties of the wave function for the valence neutron. Therefore, to some extent, our study is complementary to Ref. [16]. In addition, we also give a brief discussion on the subbarrier Coulomb dissociation of ${}^9\text{Be}$.

We introduce a microscopic $\alpha+\alpha+n$ model for ⁹Be. We first consider an intrinsic wave function as a basis where two alpha particles and the valence neutron are located at $\pm \vec{d}/2$ and \vec{R}_n against the origin, respectively. The total intrinsic wave function is fully antisymmetrized, and the single particle wave function for all the nucleons is expressed by a Gaussian function. Each α cluster contains four nucleons, and its wave function reads

$$\phi^{(\alpha)}(\vec{r}_{p\uparrow}, \vec{r}_{p\downarrow}, \vec{r}_{n\uparrow}, \vec{r}_{n\downarrow})$$

$$= G_{\vec{R}_{\alpha}}(\vec{r}_{p\uparrow})G_{\vec{R}_{\alpha}}(\vec{r}_{p\downarrow})G_{\vec{R}_{\alpha}}(\vec{r}_{n\uparrow})G_{\vec{R}_{\alpha}}(\vec{r}_{n\downarrow})\chi_{p\uparrow}\chi_{p\downarrow}\chi_{n\uparrow}\chi_{n\downarrow}, \tag{1}$$

where χ denotes the spin-isospin wave function. Here, G represents a Gaussian function,

$$G_{\vec{R}}(\vec{r}) = \frac{1}{(\pi s^2)^{3/4}} \exp[-(\vec{r} - \vec{R})^2 / 2s^2],$$
 (2)

and $\vec{R}_{\alpha} = \pm \vec{d}/2$. The wave function for the valence neutron is also expressed by a Gaussian (2) with $\vec{R} = \vec{R}_n$. The total intrinsic wave function is then projected onto the eigen-states of angular momentum J and parity, which we perform numerically. Note that for ⁹Be the MO picture can be introduced by merely performing the parity projection, since the α - α core is always an even-parity system.

The spectra of ⁹Be are obtained by superposing the basis states with different α - α distances d as well as neutron distances \vec{R}_n . The coefficients for the superposition are determined by the variational principle. To this end, we descretize \vec{R}_n , and include from zero

to $|\vec{R}_n^{\max}| = 15 \text{fm}$ with a step size of typically 2 fm. The α - α distances d and the relative angle between \vec{d} and \vec{R}_n are also discretized similarly. For the oscillator parameter in the Gaussian function (2), we use s = 1.46 fm in the following calculations. The adopted effective nucleon-nucleon interaction is the Volkov No.2 with the exchange parameters M = 0.6 (W = 0.4) for the central part, and the G3RS spin-orbit term for the spin-orbit part as in Ref. [9]. All the parameters of this interaction were determined from the $\alpha + n$ and $\alpha + \alpha$ scattering phase shifts.

Our interest in this paper is to compute the photo reaction cross sections of 9 Be. For this purpose, we assume that the 9 Be eventually breaks up to $\alpha + \alpha + n$ with 100% of probability once it is excited above the threshold for neutron emission. With this assumption, the photodisintegration cross sections are equivalent to the photo absorption cross sections. Since the calculations are based on the bound state approximation, the continuum states appear as discrete states. For unpolarized photons, using the Fermi's Golden rule, the E1 photoabsorption probability per unit time from a bound state i to f reads [17]

$$w_{i \to f}^{(E1)}(E_{\gamma}) = \frac{e^2}{2\pi} \frac{1}{3} \frac{E_{\gamma}}{\hbar} |\langle f | \vec{r} | i \rangle|^2 \delta(E_f - E_i - E_{\gamma}), \tag{3}$$

where E_{γ} is the photon energy, and E_i and E_f is the energy of the state i and f, respectively. The photo absorption cross sections are obtained by dividing the probability $w_{i\to f}^{(E1)}$ by the photon flux, $c/(2\pi)^3$,

$$\sigma_{i \to f}^{(E1)}(E_{\gamma}) = \frac{16\pi^3}{9} \frac{E_{\gamma}}{\hbar c} B(E1; i \to f) \,\delta(E_f - E_i - E_{\gamma}). \tag{4}$$

Here we have carried out the summation for different m substates for the states i and f. In order to mimic the neutron emission from the excited states of 9 Be, we smear the delta function in Eq. (4) by the Breit-Wigner function as

$$\sigma_{i \to f}^{(E1)}(E_{\gamma}) = \frac{16\pi^3}{9} \frac{E_{\gamma}}{\hbar c} B(E1; i \to f) \frac{\Gamma/2\pi}{(E_{\gamma} - E_f + E_i)^2 + \Gamma^2/4}.$$
 (5)

The total cross sections are then obtained by summing up all the final states f.

In the present model, the energy of the ground $3/2^-$ state of ${}^9\text{Be}$ and the ground 0^+ state of ${}^8\text{Be}$ is calculated as -56.3 MeV and -54.7 MeV, respectively. Since it is experimentally known that the ${}^9\text{Be}$ nucleus is bound from the ${}^8\text{Be}+n$ threshold by 1.7 MeV, the present model provides the correct binding energy for the ground state of ${}^9\text{Be}$ within 0.1 MeV accuracy, which is remarkably good. The convergence feature of the energy of the ground

TABLE I: The energy convergence of the ground $3/2^-$ state and the first $1/2^+$ state of ${}^9\text{Be}$. The Gaussian center of the valence neutron is incorporated up to $|\vec{R}_n^{\text{max}}| = \text{(I)}$: 2.5 fm, (II): 6.0 fm, (III): 10.0 fm, and (IV): 15.0 fm, measured from the center of mass of the α - α core, respectively. The energy of the 0^+ ground state of the α - α core is calculated to be -54.7 MeV. The B(E1) value from the ground $3/2^-$ state to the first $1/2^+$ state is also listed for each model space.

	$ \vec{R}_n^{\max} $ (fm)	$3/2^{-} \; ({\rm MeV})$	$1/2^+ \text{ (MeV)}$	$B(E1) (e^2 \text{ fm}^2)\uparrow$
(I)	2.5	-54.5	-50.3	0.022
(II)	6.0	-55.8	-53.1	0.032
(III)	10.0	-56.3	-54.0	0.042
(IV)	15.0	-56.3	-54.3	0.048

state as well as the unbound first $1/2^+$ state (just above the $^8\mathrm{Be}+n$ threshold) with respect to the maximum spatial separation $|\vec{R}_n^{\mathrm{max}}|$ for the valence neutron is listed in Table I, together with the corresponding B(E1) values. Here, the Gaussian center of the valence neutron is incorporated up to (I): 2.5 fm, (II): 6.0 fm, (III): 10.0 fm, and (IV): 15.0 fm, measured from the center of mass of the α - α core, respectively. Since the ground $3/2^-$ state is bound from the threshold by only 1.7 MeV and it thus has a rather long tail, we see that at least $|\vec{R}_n^{\mathrm{max}}| = 10.0$ fm is needed for the quantitative description of the ground state of $^9\mathrm{Be}$. Note that $|\vec{R}_n^{\mathrm{max}}| = 4$ fm was employed in the previous MO calculation for $^9\mathrm{Be}$ [9]. For the unbound $1/2^+$ state, the main component is the s-wave, which is free from the centrifugal barrier, and an extended model space is required. We find that the model space (IV), where the wave function of the valence neutron is solved up to 15 fm from the core, is needed to reach the convergence.

For the $\alpha + \alpha + n$ system, the E1 transition is allowed only as a consequence of the recoil effect of the α - α core caused by the valence neutron around it, since we do not introduce the effective charge. Notice that the B(E1) value is exactly zero for the α - α core without the valence neutron. Therefore, it is crucial to take a large enough model space for the valence neutron in order to obtain a quantitative prediction for the B(E1) value. The calculated B(E1) value increases by more than a factor of two when the model space is enlarged from (I) to (IV), leading to a value which is consistent with the recent experiment by Utsunomiya

TABLE II: The excitation energy and the E1 transition probability from the ground state to the excited states used to obtain the photodisintegration cross sections. The (*) denotes the resonance states. Only those states whose excitation energy is below 5 MeV are shown.

J^{π}	$E_x \text{ (MeV)}$	$B(E1)\uparrow (e^2 fm^2)$
1/2+ (*)	2.05	0.048
$1/2^{+}$	3.55	0.0062
3/2+ (*)	4.42	0.0088
$3/2^{+}$	4.91	0.018
5/2+ (*)	3.13	0.028
$5/2^{+}$	4.93	0.035

et al. $(0.054 \pm 0.004 e^2 \text{ fm}^2)$ [15].

Adopting the B(E1) value for the model space (IV), we show in Fig. 1 the photodisintegration cross sections of $^9\mathrm{Be}$ as a function of the photon energy E_γ . The experimental data are taken from Ref. [15]. Table II lists the states included in the calculation, which are obtained by the present MO method. For the width Γ in eq.(5), we used the experimental values for the first $3/2^+$ and $5/2^+$ resonance states, while we arbitrarily chose $\Gamma=1$ MeV for non-resonant continuum states. For the width for the first $1/2^+$ state, we use the energy dependent width given in Ref. [15]. The dashed line shows the results of the present calculation thus obtained. It appears that the low energy cross sections are sensitive to the energy of the lowest $1/2^+$ state as well as the B(E1) value to this state. We found that the energy of the $1/2^+$ state was rather sensitive to the box size, even after the B(E1) value was converged. Since we could not obtain the converged energy for the $1/2^+$ state with controlled numerical accuracy, we instead used the experimental value for it ($E_x=1.78$ MeV), although we used the calculated value for the B(E1) (see the solid line). Besides this point, we see that the agreement of the theoretical results with the experimental cross sections is satisfactory.

We have also applied the present calculation to the Coulomb excitations of 9 Be. In Ref. [4], it was shown that, although the energy dependence was well reproduced, the measured probability for the Coulomb excitation for the 9 Be + 208 Pb reaction were underestimated by a factor of two by a calculation which included the first $1/2^{+}$ and $5/2^{-}$ states together

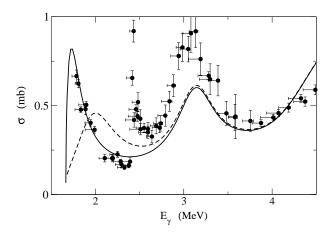


FIG. 1: The E1 photodisintegration cross sections of 9 Be as a function of photon energy obtained in the molecular orbital model (the dashed line). The experimental data are taken from Ref. [15]. The solid line is the result of the molecular orbital model but with use of the experimental energy for the lowest $1/2^{+}$ state.

with the experimental values for the excitation energies and the electromagnetic transition probabilities. The underestimation of the Coulomb excitation probability is likely attributed to the lack of non-resonant continuum states in the calculation. We therefore repeated the calculation by including the states shown in Table II. It was found, however, that the number of continuum states which we obtained by the present MO calculation was too small to resolve the discrepancy. This is certainly a limitation of the box discretization, and one would need the proper scattering boundary condition for the continuum states in order to reconcile the discrepancy.

In summary, the photodisintegration cross section of 9 Be newly measured by Utsunomiya et al. was successfully reproduced by a microscopic α -cluster model. It was found that the B(E1) transition from the ground state to the first $1/2^{+}$ state, which plays an important role in explosive nucleosynthesis, has a strong dependence on the model space for the valence neutron. Incorporating the neutron orbit up to around 15 fm from the 8 Be core, we obtained the B(E1) value consistent with the new experimental value, which is almost twice the previous measurement.

We thank H. Utsunomiya for useful discussions and providing us with the experimental data in a numerical form. K.H. thanks D.J. Hinde and M. Dasgupta for useful discussions. This work is supported in part by Grant-in-Aid for Scientific Research (13740145) from the

- [1] A. Navin, D.W. Anthony, T. Aumann, T. Baumann, D. Bazin, Y. Blumenfeld, B.A. Brown, T. Glasmacher, P.G. Hansen, R.W. Ibbotson, P.A. Lofy, V. Maddalena, K. Miller, T. Nakamura, B.V. Pritychenko, B.M. Sherrill, E. Spears, M. Steiner, J.A. Tostevin, J. Yurkon, and A. Wagner, Phys. Rev. Lett. 85, 266 (2000).
- [2] A. Bonaccorso and G.F. Bertsch, Phys. Rev. C63, 044604 (2001).
- [3] M. Dasgupta, D.J. Hinde, R.D. Butt, R.M. Anjos, A.C. Berriman, N. Carlin, P.R.S. Gomes, C.R. Morton, J.O. Newton, A. Sanzto di Toledo, and K. Hagino, Phys. Rev. Lett. 82, 1395 (1999).
- [4] D.J. Hinde, M. Dasgupta, B.R. Fulton, C.R. Morton, R.J. Wooliscroft, A.C. Berriman and K. Hagino, (to be published).
- [5] S. Okabe and Y. Abe, Prog. Theor. Phys. **61**, 1049 (1979).
- [6] P. Descouvemont, Phys. Rev. C39, 1557 (1989).
- [7] K. Arai, Y. Ogawa, Y. Suzuki, and K. Varga, Phys. Rev. C54, 132 (1996).
- [8] Y. Kanada-En'yo and H. Horiuchi, Prog. Theor. Phys. Suppl. 142, 205 (2001).
- [9] N. Itagaki and S. Okabe, Phys. Rev. C61, 044306 (2000).
- [10] N. Itagaki, S. Okabe, and K. Ikeda, Phys. Rev. C62, 034301 (2000).
- [11] N. Itagaki, S. Okabe, and K. Ikeda, Prog. Theor. Phys. Suppl. 142, 297 (2001).
- [12] N. Itagaki, S. Hirose, T. Otsuka, S. Okabe, and K. Ikeda, Phys. Rev. C65, 044302 (2002).
- [13] S.E. Woosley and R.D. Hoffman, Astrophys. J. **395**, 202 (1992).
- [14] K. Sumiyoshi, H. Utsunomiya, S. Goko, and T. Kajino, Nucl. Phys. A, in press (2002).
- [15] H. Utsunomiya, Y. Yonezawa, H. Akimune, T. Yamagata, M. Ohta, M. Fujishiro, H. Toyokawa, and H. Ohgaki, Phys. Rev. C63, 018801 (2000).
- [16] P. Descouvemont, Eur. Phys. J. A12, 413 (2001).
- [17] J.J. Sakurai, Advanced Quantum Mechanics, (Addison-Wesley Pub. Co., Reading, 1967).